

An Evaluation of Particle Swarm Optimization Techniques in Segmentation of Biomedical Images

Salim Lahmiri
Dept. of Computer Science, UQAM
Montreal, Canada
Lahmiri.salim@courrier.uqam.ca

Mounir Boukadoum
Dept. of Computer Science, UQAM
Montreal, Canada
Boukadoum.mounir@uqam.ca

ABSTRACT

Image segmentation is a common image processing step to many computer vision applications with the purpose to segment pixels into different classes. As improved variants of particle swarm optimization (PSO) algorithms, the fractional-order Darwinian particle swarm optimization (FODPSO) and Darwinian particle swarm optimization (DPSO) have been proposed for image segmentation. The purpose of this paper is to compare the segmentation performance of PSO, DPSO, and FODPSO as parametric approaches to existing methods; namely the parametric fuzzy *c*-means (FCM) algorithm, and the non-parametric Otsu segmentation technique with application to five biomedical images. All PSO-based experiments are conducted with twenty runs to assess the effectiveness of PSO models. The universal quality index is used to evaluate the segmentation results. The obtained experimental results showed that particle swarm based algorithms outperformed both FCM and Otsu segmentation technique.

Categories and Subject Descriptors

I.4.6 [Image processing and computer vision]: Segmentation.

General Terms

Algorithms; Experimentation.

Keywords

Particle swarm optimization; Fuzzy *c*-Means; Otsu technique; Segmentation; Biomedical images.

1. INTRODUCTION

In image processing and computer vision, image segmentation is a fundamental problem with the objective to partition an image into several subregions with homogeneous properties. The problem of image segmentation has received a large attention in biomedical applications [1]-[3]. Indeed, the automatic segmentation of biomedical images is a critical step for quantifying the changes of anatomical structures that are highly related to biological tissue diseases. For instance, global thresholding based on minimum cross entropy was adopted in [1] as a segmentation method for cuboidal cell nuclei in images of prostate tissue stained with hematoxylin and eosin, an atlas-aided fuzzy *c*-means (FCM-Atlas) was developed and validated in [2] to segment fibroglandular tissue and volumetric density estimation in breast MRI, and a sparse representation was adopted in [3] to fuse the multi-

modality image information and incorporate the anatomical constraints for brain tissue segmentation.

Image thresholding approaches are widely used for image segmentation [4]. They can be classified into two types: optimal thresholding methods and property based thresholding methods.

Optimal thresholding methods search for the optimal thresholds by optimizing an objective function, whilst property-based thresholding methods detect the thresholds by measuring some property of the histogram [4]. Optimal thresholding methods find the thresholds that separate the gray-level regions of an image based on some discriminating criteria such as the between-class variance, entropy and cross entropy [5]. For instance, the popular Otsu's unsupervised method [6] selects optimal thresholds by maximizing the between class variance.

In general, optimal thresholding methods are simple and effective in bi-level thresholding [7]. However, they are; including Otsu's unsupervised method; inefficient in determining the optimal thresholds due to the exponential growth in computation time in when dealing with multilevel thresholding problems [7]. As an alternative, some evolutionary techniques have been adopted to solve multilevel thresholding problems; including bacterial foraging algorithm [7], particle swarm optimization [4][8], ant colony optimization [9], and more recently the fractional-order Darwinian particle swarm optimization (FODPSO) and Darwinian particle swarm optimization (DPSO) [10].

Because of its effectiveness, PSO based algorithms have received increasing interests in image segmentation [4][8][10] including its extensions; namely FODPSO and Darwinian particle swarm optimization DPSO. In [10], the DPSO and FODPSO were proposed for solving the Otsu problem for delineating multilevel threshold values. In particular, the problem of *n*-level thresholding is reduced to an optimization problem to search for the thresholds that maximizes a set of three objective (fitness) functions of each RGB (red-green-blue) component of the image [10]. The obtained results indicated that FODPSO is more efficient than PSO, DPSO, bacteria foraging algorithm, and genetic algorithms in the problem of segmentation of five images: airplane, hunter, butterfly, road, and a map.

The purpose of this study is to examine the effectiveness of PSO, DPSO, and FODPSO in the problem of biomedical image segmentation. Indeed, the task of determining optimal thresholds for *n*-level image thresholding could be formulated as a multidimensional optimization problem by using PSO-based models [10]. As a result, optimal thresholds are automatically determined by using PSO-based algorithms. For comparison purpose, the popular Otsu's unsupervised method [6] and fuzzy *c*-means (FCM) algorithm [11] are also used for segmentation of biomedical images used in our study. The FCM is chosen because it is more appropriate for data clustering when the boundaries

Permission to make digital or hard copies of all or part of this work for personal or classroom use is granted without fee provided that copies are not made or distributed for profit or commercial advantage and that copies bear this notice and the full citation on the first page. Copyrights for components of this work owned by others than ACM must be honored. Abstracting with credit is permitted. To copy otherwise, or republish, to post on servers or to redistribute to lists, requires prior specific permission and/or a fee. Request permissions from permissions@acm.org.
GECCO'14, July 12–16, 2014, Vancouver, BC, Canada.
Copyright is held by the owner/author(s). Publication rights licensed to ACM.
ACM 978-1-4503-2881-4/14/07...\$15.00.
<http://dx.doi.org/10.1145/2598394.2609855>

between data clusters are ill defined [12]. We notice that Otsu's approach is nonparametric since it requires no predetermined parameters, whilst FCM is parametric because the number of clusters should be set a priori. Finally, the performance of each algorithm is evaluated based on the well known universal quality index [13]. It is independent of the images being tested, the viewing conditions or the individual observers [13]. In addition, it provides a meaningful comparison across different types of image distortions [13]. Jaccard index and Dice similarity index are not considered in this study since the former is more suitable for binary images, and the latter is sensitive to homogenous data.

The rest of this paper is organized as follows. In Section 2, PSO, DPSO, FCM, Otsu technique, and the universal quality index are described. In Sections 3, results of biomedical images are presented. Finally, we conclude in Section 4.

2. METHODS

2.1 Particle Swarm Optimization

In basic PSO, a swarm of individuals, called particles, collectively moves in the search space, with each particle position representing a candidate solution to the optimization problem at hand. During the search, each particle adjusts its motion according to the best position it achieved as well as to the best ones achieved by the swarm. A fitness function is used to evaluate particle performance at each step.

In the context of image segmentation, the pixel set corresponds to the search space, and the optimal solution corresponds to maximizing the between-class (between objects in the image) variance of the distribution of intensity levels in the image. Following the notation in [10] notation, at time t each particle n moves in a search space with position x_t^n and velocity v_t^n which are dependent on local best position \tilde{x}_t^n neighborhood best \tilde{n}_t^n and global best \tilde{g}_t^n information as follows:

$$v_{t+1}^n = wv_t^n + \rho_1 r_1 (\tilde{g}_t^n - x_t^n) + \rho_2 r_2 (\tilde{x}_t^n - x_t^n) + \rho_3 r_3 (\tilde{n}_t^n - x_t^n) \quad (1)$$

$$x_{t+1}^n = x_t^n + v_{t+1}^n \quad (2)$$

where the parameters w , ρ_1 , ρ_2 , and ρ_3 are respectively the weights of the inertial influence, global best, local best, and neighborhood best when determining the new velocity [10]. The parameters r_1 , r_2 , and r_3 are vectors with uniform random numbers between 0 and 1 associated to each component of Equation 2. The fitness function φ used to evaluate the performance of the particles is given by [10]:

$$\varphi = \max_{1 < t_1 < \dots < t_{n-1} < L} \sigma(t_j) \quad (3)$$

where, σ is the between-class variance of the image intensity distributions, t is a given threshold, L is the intensity level, and n is the number of classes into which the pixels of the image are divided (by grouping pixels in terms of their gray levels been within a specified range). More details about the fitness function are found in [10].

The PSO algorithm is summarized in Table 1 [10]. A certain number of parameters must be initialized before running it. Typically, the particle velocities are set to zero and their positions are randomly set within the boundaries of the image number of intensity levels L . For instance, the positions can be initialized as $\eta(L - X_{\min}) + X_{\min}$, where η is a random variable in $[0,1]$ and X_{\min} is a predetermined parameter. In addition, the local best, neighborhood best and global best positions are initialized with the worst possible values [10], e.g., large negative numbers. As for the particle population size and iteration stopping criterion, they can be arbitrarily set or chosen depending on the nature of the problem and/or data.

Table 1. Algorithm of the PSO as in [10]

Initialize swarm: $x_t^n, v_t^n, \tilde{x}_t^n, \tilde{n}_t^n, \tilde{g}_t^n$
Loop:
For all particles
Evaluate the fitness φ of each particle
Update : $x_t^n, \tilde{n}_t^n, \tilde{g}_t^n$
Update : v_t^n, \tilde{x}_t^n
End
Until stopping criteria (convergence) reached

2.2 Darwinian Particle Swarm Optimization

One drawback of the PSO algorithm described in Table 1 is that it may get stuck in a sub-optimal solution region [10][14]. To avoid this situation, Tillett et al, [14] introduced the Darwinian particle swarm optimization (DPSO), an extension of the algorithm that uses natural selection to escape from local optima. In particular, the classic PSO is extended to multiple swarms where each one performs a PSO search. Thus, many swarms of test solutions coexist. At each step, a swarm that gets better results is allowed to spawn a new descendent or a particle life is extended. On the contrary, a swarm life is reduced or its particles are reduced in number if it stagnates. The state of each swarm is evaluated based on the fitness of all its particles, and the neighborhood and individual best positions of each of the particles are updated. Then, a new particle is spawned if a new global solution is found. In particular, if the swarm population falls below a minimum bound, the swarm is deleted; and the worst performing particle in the swarm is deleted if a maximum threshold number of steps (SC_C^{\max}) is reached without improving the fitness function. The previous steps counter is reset to a value approaching the threshold number if the particle is deleted, as follows [14]:

$$SC_c(N_{kill}) = SC_C^{\max} \left(1 - \frac{1}{N_{kill} + 1} \right) \quad (4)$$

where N_{kill} is the number of particles deleted from the swarm when there is no improvement in fitness during an iteration. A new swarm is created with a probability of $p=f/S$, with f is a random number in $[0,1]$ and S is the number of swarms [10]. Finally, a set of initial parameters is determined to run the DPSO algorithm; including the initial swarm population, minimum and maximum swarm population, initial number of swarms, minimum and maximum number of swarms, and the image number of

threshold. The algorithm of the DPSO is presented in Table 2 as in [10].

Table 2. Algorithm of the DPSO as in [10]

Main program loop	Evolve swarm algorithm
For each swarm in the collection	For each particle in the swarm
Evolve the swarm (see right column)	Update particle Fitness
Allow the swarm to spawn	Update particles Best
Delete failed swarms	Move particle
	If swarm gets better
	Reward swarm: spawn particle:
	extend swarm life
	else
	Punish swarm: possibly delete
	particle: reduce swarm life

2.3 Fractional-order Darwinian Particle Swarm Optimization

Recently, the authors in [15] presented fractional-order (FO) DPSO or FODPSO. The idea was to use fractional calculus based on the Grünwald-Letnikov concept of fractional differential [16] to control the convergence rate of the DPSO. The fractional differential α of a given signal $x(t)$ is given by:

$$D^\alpha [x(t)] = \frac{1}{T^\alpha} \sum_{k=0}^r \frac{(-1)^k \Gamma(\alpha+1) x(t-kT)}{\Gamma(k+1) \Gamma(\alpha-k+1)} \quad (5)$$

where Γ , T , and r are respectively the gamma function, the sampling period, and the truncation order. Then, considering $w=1$, $T=1$, and $r=4$, the differential derivative of Equation 1 is written as [15][17]:

$$v_{t+1}^n = \alpha v_t^n + \frac{1}{2} \alpha v_t^n + \frac{1}{6} \alpha (1-\alpha) v_{t-2}^n + \frac{1}{24} \alpha (1-\alpha) (2-\alpha) v_{t-3}^n + \rho_1 r_1 (\tilde{g}_t^n - x_t^n) + \rho_2 r_2 (\tilde{x}_t^n - x_t^n) + \rho_3 r_3 (\tilde{n}_t^n - x_t^n) \quad (6)$$

Thus, setting $\alpha=1$ yields the standard DPSO. The parameter is closely related to the memory of the particles. If $\alpha < 1$, the particles will ignore their previous search and will probably be trapped in local solutions, whilst if $\alpha > 1$, the particles will explore more new solutions and performance will be improved [10]. The FODPSO was found to be more efficient than PSO and DPSO when the level of segmentation increases [10].

Table 3 provides the parameter values used to perform PSO, DPSO, and FODPSO searches in our study. These are the same as in [10], since they provided good results with fast processing time.

Table 3. Initial parameters as in [10]

Parameter	PSO	DPSO	FODPSO
Number of iterations	150	150	150
Population	150	30	30
ρ_1	0.8	0.8	0.8
ρ_2	0.8	0.8	0.8
w	1.2	1.2	1
V_{\min}	-5	-1.5	-1.5
V_{\max}	5	1.5	1.5
X_{\min}	0	0	0
X_{\max}	255	255	255
Min population		10	10
Max population		50	50
Number of swarms		4	4
Min swarms		2	2
Max swarms		6	6
Number of threshold		10	10
Fractal coefficient α			0.6

2.4 Fuzzy c-Means Clustering

The fuzzy c-means clustering (FCM) algorithm [11] also classifies a given data set into k clusters, but it realizes a fuzzy partition. It does so by minimizing the following objective function:

$$J_{FCM} = \sum_{j=1}^K \sum_{i=1}^N u_{ij}^m \|x_i^j - c_j\|^2 \quad (7)$$

where x and c stand respectively for the position of pixel i and the centroid of cluster j , N is the number of pixels, and K is the number of cluster, u_{ij} is a membership function, $j=1, \dots, N$, and $m \in [1, \infty)$ identifies a fuzzifier [11]. Thus, the data points are partitioned into fuzzy regions using fuzzy membership grades [12]. The FCM must satisfy the constraint:

$$\sum_{j=1}^N u_{ij} = 1 \quad (8)$$

and the centroid of cluster j is calculated as follows:

$$c_j = \sum_{i=1}^N \frac{u_{ij}^m}{\sum_{k=1}^N u_{ik}^m} \quad (9)$$

Finally, the membership u_{ij} is updated as follows:

$$u_{ij} = \frac{\|x_j - c_j\|^{-1/(m-1)}}{\sum_{i=1}^c \|x_j - c_j\|^{-1/(m-1)}} \quad (10)$$

The role of the membership functions is to introduce fuzziness to the belongingness of each image pixel. As a result, each pixel belongs to all clusters, but with different degrees of membership.

2.5 Otsu Segmentation Approach

The Otsu segmentation method [6] is a threshold selection technique used to segment gray-level images by maximizing the following measure of class separability [18]:

$$D(T) = \frac{P_1(T)P_2(T)[m_1(T) - m_2(T)]^2}{P_1(T)\sigma_1^2(T) + P_2(T)\sigma_2^2(T)} \quad (11)$$

where,

$$P_1(T) = \sum_{z=0}^T h(z) \quad (12)$$

$$P_2(T) = 1 - P_1(T) \quad (13)$$

$$m_1(T) = \frac{1}{P_1(T)} \sum_{z=0}^T zh(z) \quad (14)$$

$$m_2(T) = \frac{1}{P_2(T)} \sum_{z=T+1}^{L-1} zh(z) \quad (15)$$

$$\sigma_1(T) = \frac{1}{P_1(T)} \sum_{z=0}^T [z - m_1(T)]^2 h(z) \quad (16)$$

$$\sigma_2(T) = \frac{1}{P_2(T)} \sum_{z=T+1}^{L-1} [z - m_2(T)]^2 h(z) \quad (17)$$

where, $z \in [0, L-1]$ is the grey-level of a pixel in the image, $h(z)$ is the normalized grey-level histogram of the image. The means of the light and dark image regions can be separated, and the variances of the two image regions can be minimized when $D(T)$ is maximized.

2.6 Evaluation Metric

For two signals $x=1, \dots, N$ and $y=1, \dots, N$ which are respectively the original and the test signal, the universal quality index Q [13] is given by:

$$Q = \frac{4\sigma_{xy}\bar{x}\bar{y}}{(\sigma_x^2 + \sigma_y^2) + (\bar{x}^2 + \bar{y}^2)} \quad (18)$$

Where \bar{x} , \bar{y} , σ_x , σ_y , and σ_{xy} are respectively the mean of x , mean of y , standard deviation of x , standard deviation of y , and the correlation coefficient between x and y . Alternatively, the quality index Q can be rewritten as a product of three components as follows:

$$Q = \frac{\sigma_{xy}}{\sigma_x\sigma_y} \cdot \frac{2\bar{x}\bar{y}}{\bar{x}^2 + \bar{y}^2} \cdot \frac{2\sigma_x\sigma_y}{\sigma_x^2 + \sigma_y^2} \quad (19)$$

where the first component is the correlation coefficient used to measure the degree of linear correlation between the two signals, the second component measures how close the mean luminance is between the two signals, and the third component measures how

similar the contrasts of the images are [13]. For images, the quality index Q is computed as follows:

$$Q = \frac{1}{M} \sum_{i=1}^M Q_i \quad (20)$$

where M is the number of steps used to slide a window of size $B \times B$ which in turns moves pixel by pixel horizontally and vertically through all the rows and columns from the top-left to the bottom-right corner.

3. DATA AND RESULTS

In the present study we have used the five biomedical images: T1-weighted whole view of brain magnetic resonance image (MRI) (176×208 pixels), T1-weighted coronal view of brain MRI (176×176 pixels), T1-weighted sagittal view of brain MRI (208×176 pixels), prostate biological tissue (275×183 pixels), and breast biological tissue (631×471 pixels). They are respectively shown in Figures 1, 2, 3, 4, and 5. Since PSO and its variants are stochastic models, we performed twenty runs on each image and average and standard deviation of the universal quality index are computed. Table 4 shows the obtained results. The segmentation results are illustrated in Figures 6 to 20. Those of brain whole and coronal view are not shown because of limited space.

As indicated in Table 4, all PSO based algorithms outperformed FCM and Otsu technique in segmentation of all five images. In addition, the results indicated that PSO outperforms both DPSO and FODPSO in segmentation of prostate and breast tissue. They all obtained similar universal quality index value when used to segment brain sagittal view. Finally, both DPSO and FODPSO achieved the same performance and outperformed basic PSO when applied to the whole view of brain MRI.

In general, the obtained results are not consistent with [10] since we find that PSO outperforms both DPSO and FODPSO in segmentation of prostate and breast tissue.

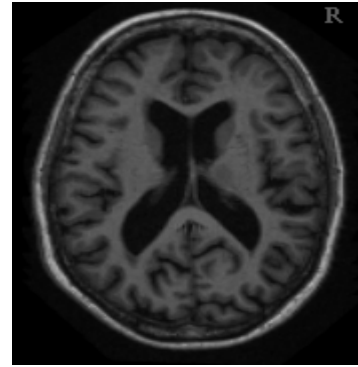


Figure 1. Whole brain MRI.

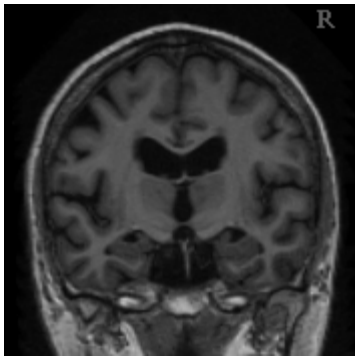


Figure 2. Coronal view of brain MRI.

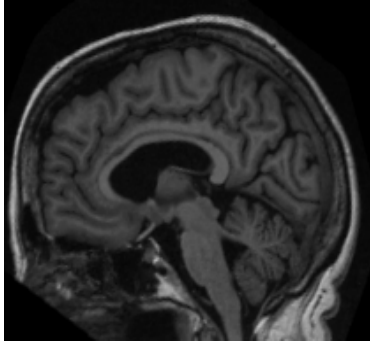


Figure 3. Sagittal view of brain MRI.

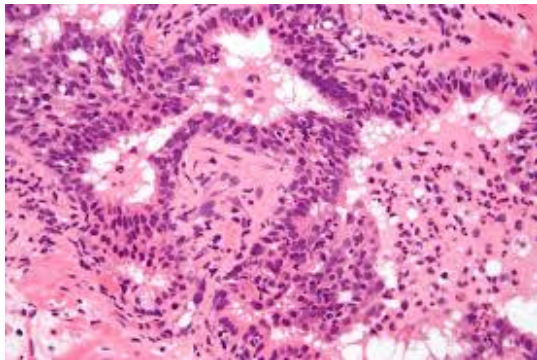


Figure 4. Prostate biological tissue.

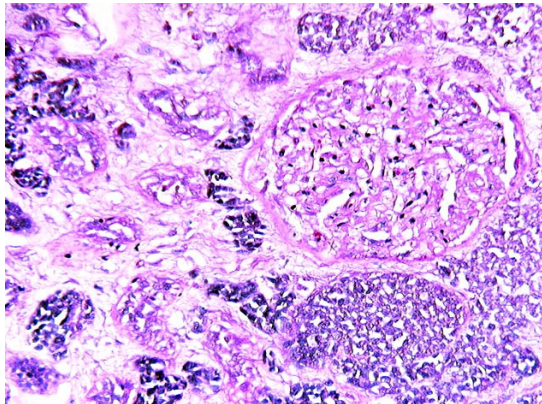


Figure 5. Breast biological tissue.

Table 4. Obtained universal quality index

	PSO	DPSO	FODPSO	FCM	OTSU
Brain Whole view	0.47±0.002	0.5±0.002	0.5±0.002	0.24	0.24
Brain Coronal view	0.53±0.002	0.53±0.002	0.53±0.002	0.24	0.05
Brain Sagittal view	0.53±0.002	0.53±0.002	0.53±0.002	0.04	0.04
Prostate	0.74±0.001	0.74±0.001	0.74±0.001	0.36	0.20
Breast	0.74±0.001	0.74±0.001	0.74±0.001	0.45	0.23

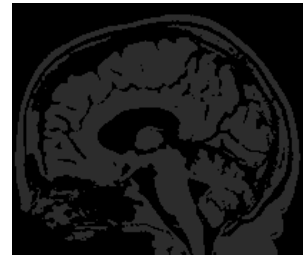


Figure 6. Sagittal view: PSO result.

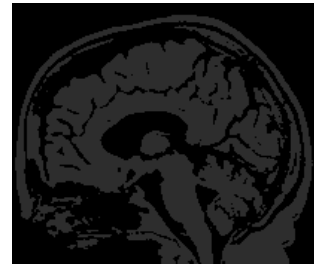


Figure 7. Sagittal view: DPSO result.

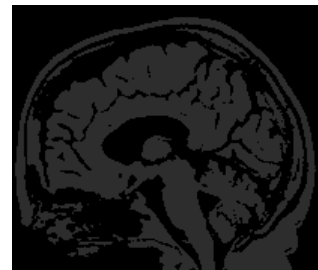


Figure 8. Sagittal view: FODPSO result.

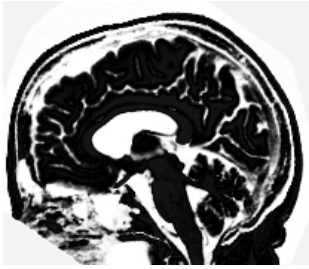


Figure 9. Sagittal view: FCM result.

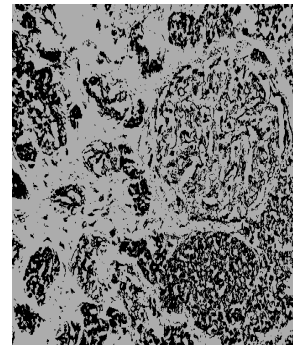


Figure 12. Prostate tissue: DPSO result.

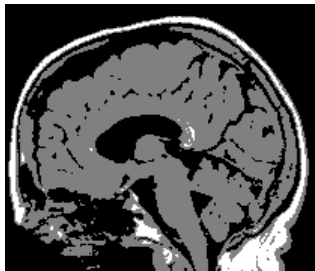


Figure 10. Sagittal view: Otsu result.

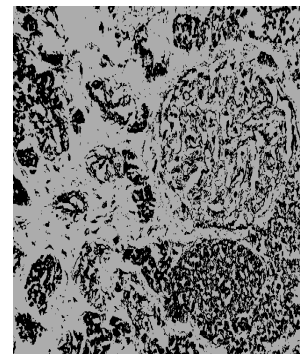


Figure 13. Prostate tissue: FODPSO result.

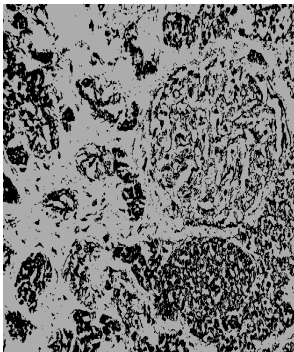


Figure 11. Prostate tissue: PSO result.

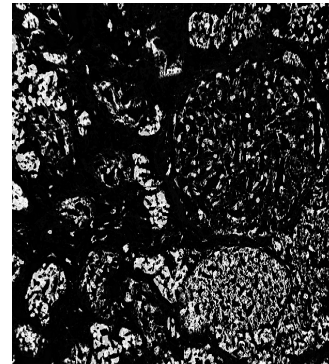


Figure 14. Prostate tissue: FCM result.

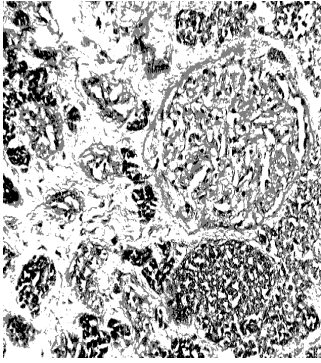


Figure 15. Prostate tissue: Otsu result.

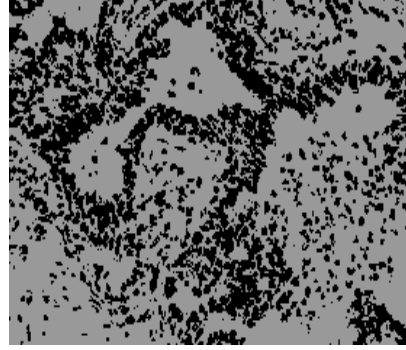


Figure 18. Breast tissue: FODPSO result.

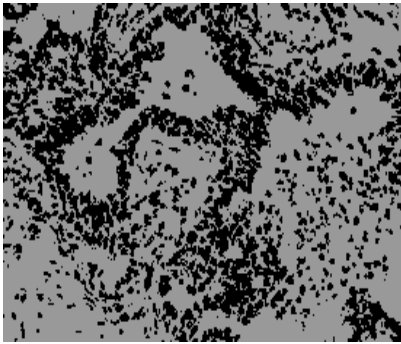


Figure 16. Breast tissue: PSO result.

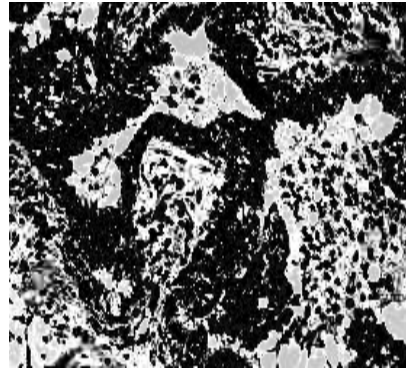


Figure 19. Breast tissue: FCM result.

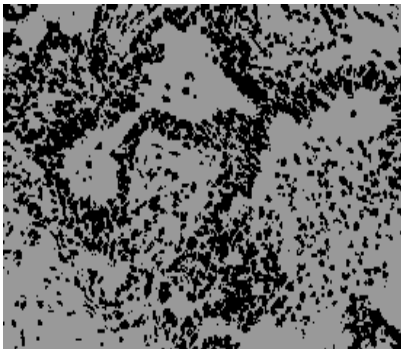


Figure 17. Breast tissue: DPSO result.

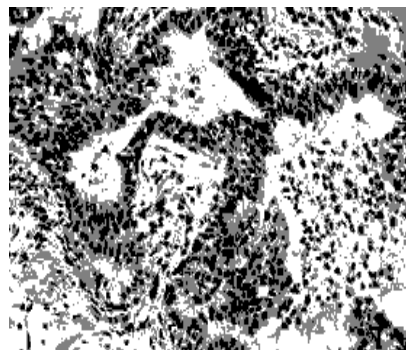


Figure 20. Breast tissue: Otsu result.

4. CONCLUSION

This study compared the performance of PSO, DPSO, FODPSO, FCM, and Otsu technique when they are used to segment different types of biological images. The main advantage of PSO, DPSO, and FODPSO is their ability to automatically determine the optimal thresholds for n -level image thresholding by formulating a multidimensional optimization problem. Based on the universal quality index used as performance measure, the obtained results indicated that all PSO based algorithms outperformed FCM and Otsu technique. In addition, the results indicated that in general PSO, DPSO, and FODPSO achieved similar performance. Therefore, this result suggests that the complexity of DPSO and FODPSO does not necessarily yield to large improvement in segmentation results of biomedical images.

Our future work will consider a comparison of PSO based algorithms with other evolutionary techniques. As our initial database was limited to five biomedical images, we will consider a larger database in future work for better generalization of the results.

5. REFERENCES

- [1] de Oliveira, D.L.L., do Nascimento M.Z., Neves, L.A., de Godoy, M.F., de Arruda, P.F.F., and de Santi Neto, D. Unsupervised segmentation method for cuboidal cell nuclei in histological prostate images based on minimum cross entropy. *Expert Systems with Applications* 40 (2013), 7331–7340.
- [2] Wu, S., Weinstein, S.P., Conant, E.F, and Kontos D. Automated fibroglandular tissue segmentation and volumetric density estimation in breast MRI using an atlas-aided fuzzy C-means method. *Med Phys.* 40 (2013); DOI: 10.1118/1.4829496.
- [3] Wang, L., Shi, F., Gao, Y., Li, G., Gilmore, J.H., Lin, W., and Shen, D. Integration of sparse multi-modality representation and anatomical constraint for iso-intense infant brain MR image segmentation. *NeuroImage* 89 (2014) 152–164.
- [4] Chander, A., Chatterjee, A., and Siarry, P. A new social and momentum component adaptive PSO algorithm for image segmentation. *Expert Systems with Applications* 38 (2011) 4998–5004.
- [5] Horng, M.-H. Multilevel thresholding selection based on the artificial bee colony algorithm for image segmentation. *Expert Systems with Applications* 38 (2011) 13785–13791.
- [6] Otsu, N. A threshold selection method from gray-level histograms. *IEEE Transactions on Systems, Man, Cybernetics, SMC-9* (1979) 62–66.
- [7] Sathya, P.D., and Kayalvizhi, R. Optimal multilevel thresholding using bacterial foraging algorithm. *Expert Systems with Applications* 38 (2011) 15549–15564.
- [8] Maitra, M., and Chatterjee, A. A hybrid cooperative-comprehensive learning based PSO algorithm for image segmentation using multilevel thresholding. *Expert Systems with Applications* 34 (2008) 1341–1350.
- [9] Zhiwei, Y., Zhaobao, Z., Xin, Y., and Xiaogang, N. Automatic threshold selection based on ant colony optimization algorithm. In *Proceedings of the International Conference on Neural Networks and Brain*, Beijing, China, Number 728–732, 2006.
- [10] Ghamisi, P., Couceiro, M.S., Benediktsson, and Ferreira, N.M.F. An efficient method for segmentation of images based on fractional calculus and natural selection. *Expert Systems with Applications* 39 (2012) 12407–12417.
- [11] Bezdek, J.C. 1981. Pattern recognition with fuzzy objective function algorithms. New York: Plenum Press.
- [12] Nefti, S., and Oussalah, M. Probabilistic-fuzzy clustering algorithm. In *Proceedings of IEEE International Conference on Systems, Man, and Cybernetics*, 4786–4791, 2004.
- [13] Wang, Z., and Bovik, A.C. A universal image quality index. *IEEE Signal Processing Letters* 9 (2002) 81–84.
- [14] Tillett, J., Rao, T.M., Sahin, F., Rao, R., and Brockport, S. Darwinian particle swarm optimization. In *Proceedings of The 2nd Indian International Conference on Artificial Intelligence* (2005) 1474–1487.
- [15] Couceiro, M.S., Ferreira, N.M.F., and Machado, J.A.T. In fractional order Darwinian particle swarm optimization. In *Proceedings of Symposium on Fractional Signals and Systems*, 2011.
- [16] Podlubny, I. 1999. Fractional differential equations. An introduction to fractional derivatives, fractional differential equations, to methods of their solution and some of their applications. Academic Press, San Diego, CA.
- [17] Couceiro, M.S., Rocha, R.P., Ferreira, N.M.F., and Machado, J.A.T. Introducing the fractional-order Darwinian PSO. In *Proceedings of SIViP* (2012) 343–350. DOI 10.1007/s11760-012-0316-2.
- [18] Yan, H. Unified formulation of a class of image thresholding techniques. *Pattern Recognition* 29 (1996) 2025–2032.